

Supporting Information:

Isomeric Product Detection in the Heterogeneous Reaction of Hydroxyl Radicals with Aerosol Composed of Branched and Linear Unsaturated Organic Molecules

Theodora Nah^{1,2}, Haoifei Zhang^{2,3}, David R. Worton^{3,4}, Christopher R. Ruehl², Benjamin B. Kirk², Allen H. Goldstein^{3,5,6}, Stephen R. Leone^{1,2,7}, and Kevin R. Wilson^{2,*}

¹Department of Chemistry, University of California, Berkeley, CA 94720, USA

²Chemical Sciences Division, Lawrence Berkeley National Laboratory, Berkeley, CA 94720, USA

³Department of Environmental Science, Policy, and Management, University of California, Berkeley, CA 94720, USA.

⁴Aerosol Dynamics Inc., Berkeley, CA 94710

⁵Environmental and Energy Technologies Division, Lawrence Berkeley National Laboratory, Berkeley, CA 94720, USA.

⁶Department of Civil and Environmental Engineering, University of California, Berkeley, CA 94720, USA.

⁷Department of Physics, University of California, Berkeley, CA 94720, USA

* To whom correspondence should be addressed: krwilson@lbl.gov

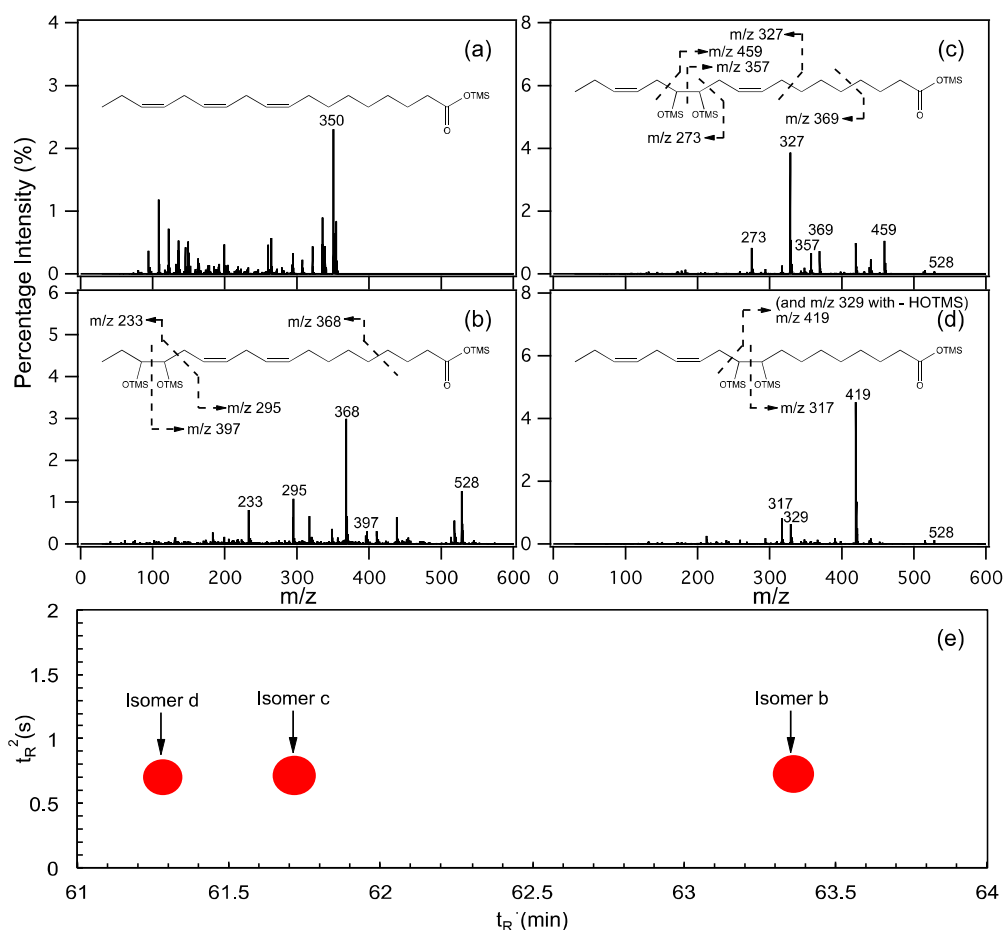


Figure S1: VUV mass spectra for (a) TMS-derivatized linolenic acid ($C_{17}H_{29}CO(OTMS)$, m/z 350), and (b – d) its TMS-derivatized diol product isomers ($C_{17}H_{29}CO(OTMS)_3$, m/z 528). Figure insets in panels (b – d) show the ion fragmentation patterns that explain the characteristic

ion peaks observed in the mass spectra of the derivatized diol product isomers. In panel (b), the ion peak at m/z 368 is formed by fragmentation and H rearrangement. (e) The relative abundance of $C_{17}H_{29}CO(OTMS)_3$ diol isomers formed during reaction at 10 % $[O_2]$ shown in GC \times GC space (t_R^1 vs. t_R^2). Each circle represents a single isomer and its relative abundance is represented by the size of the circle. Isomer b has OTMS groups on C15 and C16 of the linolenic acid backbone (mass spectrum in panel b). Isomer c has OTMS groups on C12 and C13 of the linolenic acid backbone (mass spectrum in panel c). Isomer d has OTMS groups on C9 and C10 of the linolenic acid backbone (mass spectrum in panel d).

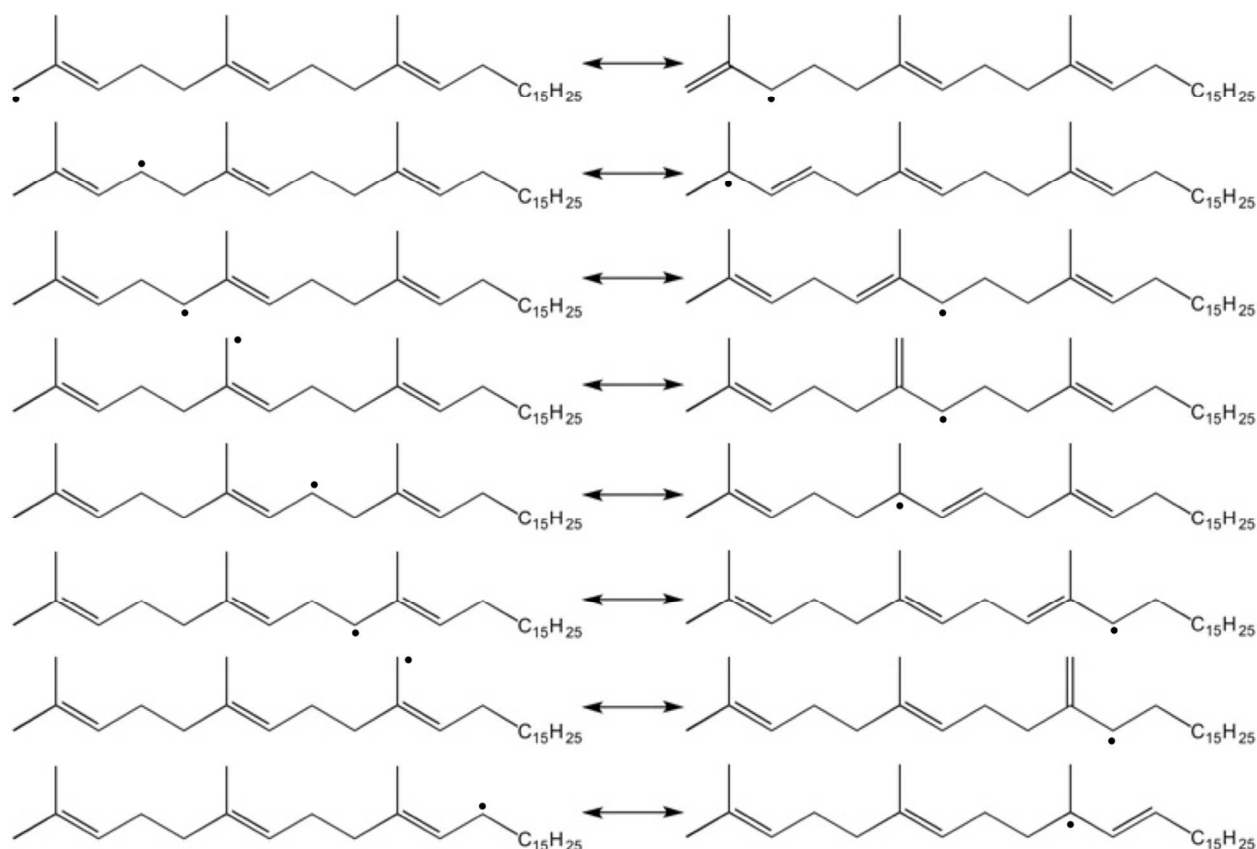


Figure S2: Structures of all 16 possible resonance-stabilized allylic R radicals formed from H atom abstraction reactions during squalene oxidation.

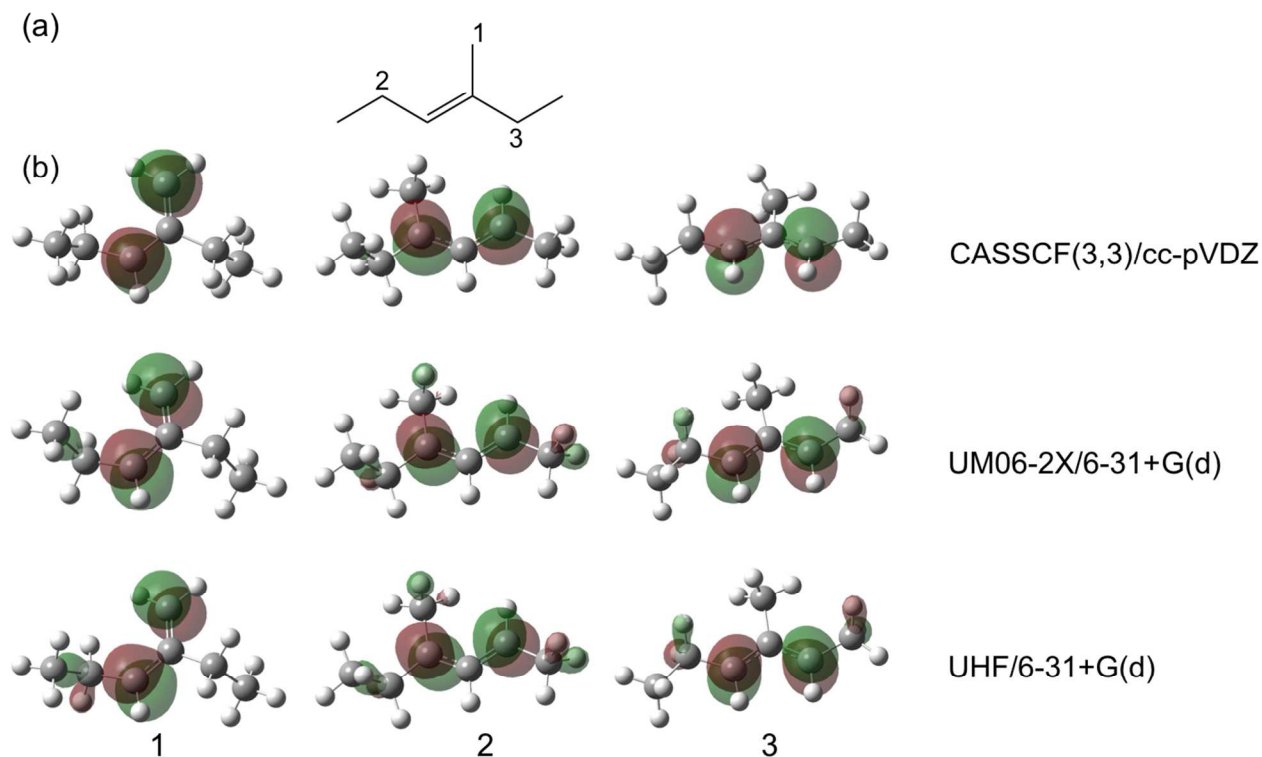


Figure S3: (a) The alkene used in spin density calculations. The carbon sites at which H atoms are abstracted from to form the allylic alkyl radicals are indicated. (b) Singly occupied molecular orbitals of the allylic alkyl radicals formed from H atom abstraction reactions computed using the Gaussian 09 program at three levels of theory (from top to bottom): the complete active space self-consistent field method CASSCF(3,3)/cc-pVDZ using an active-space of three electrons in the three π -valence orbitals; the hybrid density functional method UM06-2X/6-31+G(d); and the unrestricted hartree fock method UHF/6-31+G(d). In each case, a geometry optimization is undertaken and confirmed to be a minimum by a frequency calculation that resulted in no imaginary frequencies. The singly occupied molecular orbitals are drawn using the GaussView software package.

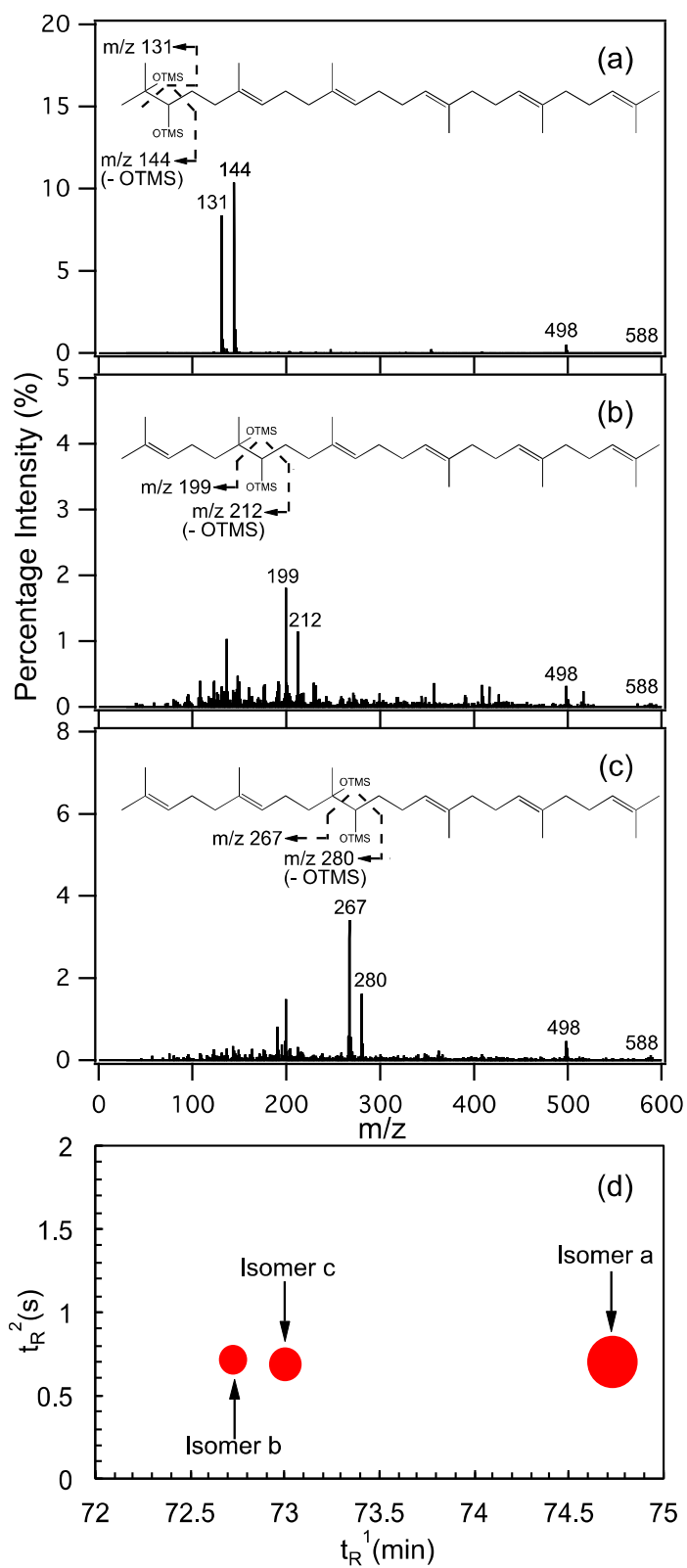


Figure S4: VUV mass spectra of the TMS-derivatized $C_{30}H_{50}(OTMS)_2$ diol product isomers (m/z 588). Figure insets in panels (a – c) show the ion fragmentation patterns that explain the

characteristic ion peaks observed in the mass spectra. In panels (a – c), the m/z 498 fragment ion is formed from the loss of HOTMS. (d) The relative abundance of $C_{30}H_{50}(OTMS)_2$ diol isomers formed during reaction at $\sim 1\%$ $[O_2]$ shown in GC \times GC space (t_R^1 vs. t_R^2). Each circle represents a single isomer and its relative abundance is represented by the size of the circle. Isomer a has OTMS groups on C2 and C3 of the squalene backbone (mass spectrum in panel a). Isomer b has OTMS groups on C6 and C7 of the squalene backbone (mass spectrum in panel b). Isomer c has OTMS groups on C10 and C11 of the squalene backbone (mass spectrum in panel c).

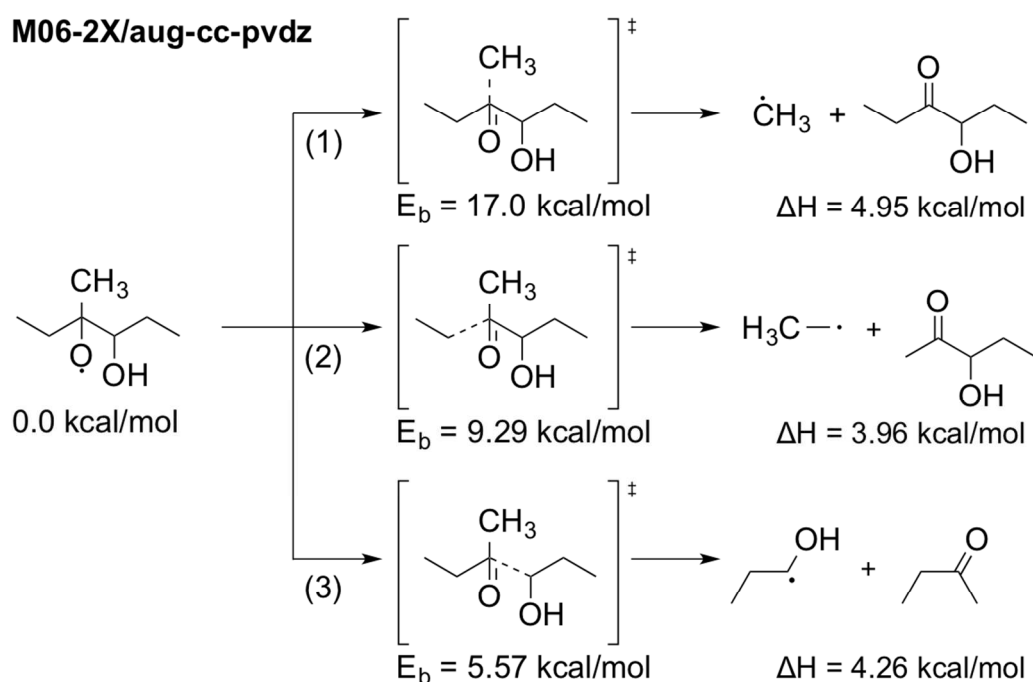


Figure S5: Barrier heights (E_b) and enthalpies (ΔH) of the three possible fragmentation reaction pathways undertaken by a tertiary hydroxyalkoxy radical. These are calculated using the Gaussian 09 program at the M06-2X level with the aug-cc-pvdz basis set.

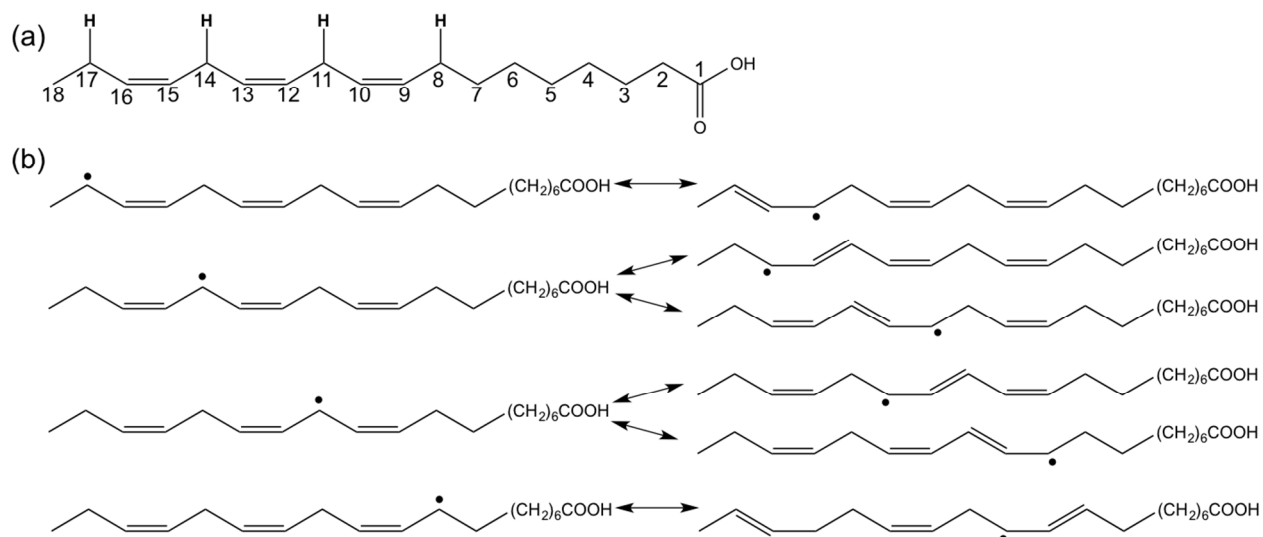


Figure S6: (a) Allylic H atoms (bold) present in linolenic acid (located at C8, C11, C14 and C17 of the carbon backbone). (b) Structures of all 10 possible resonance-stabilized allylic R radicals formed from H atom abstraction reactions during linolenic acid oxidation.

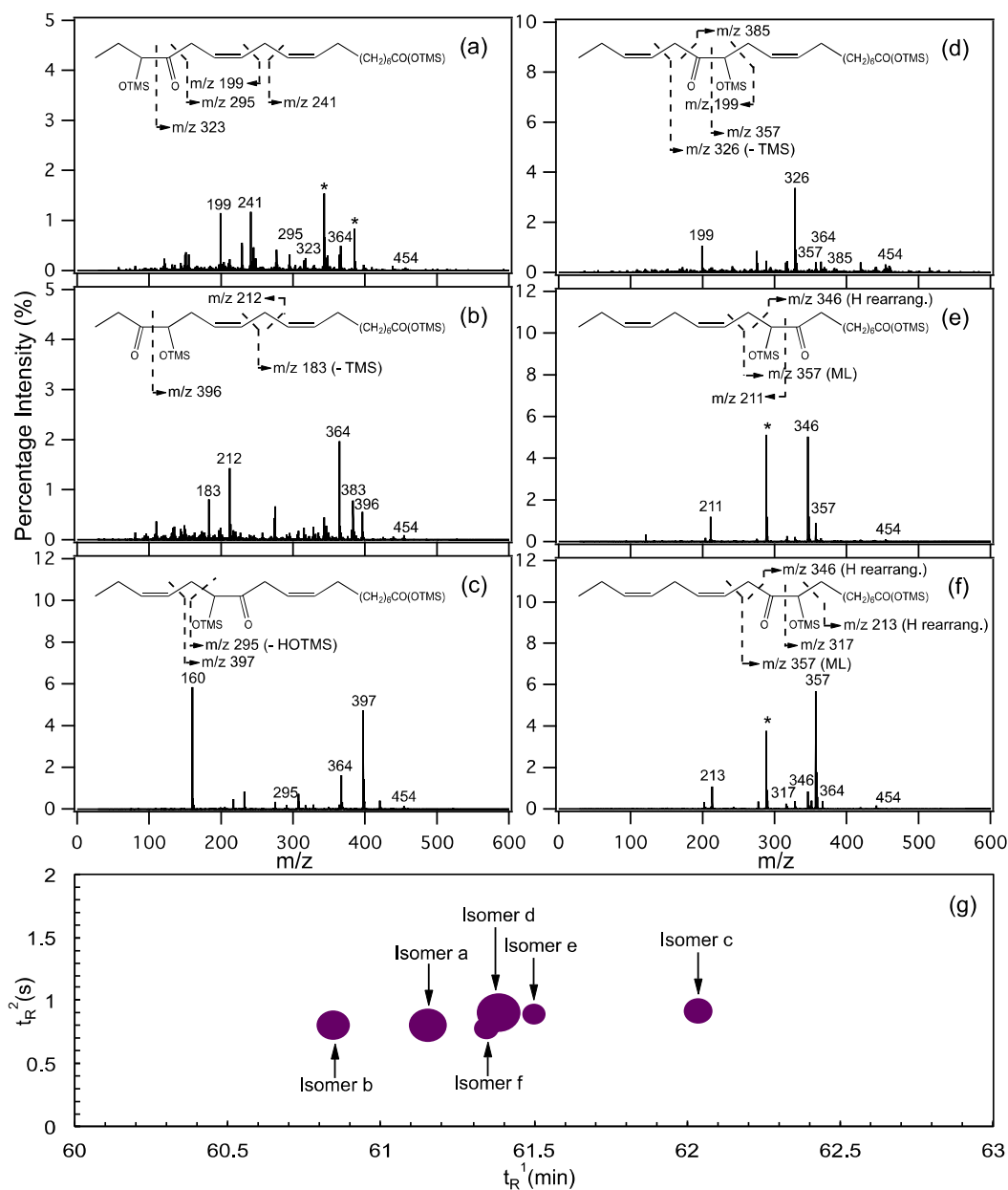


Figure S7: VUV mass spectra for the TMS-derivatized $C_{17}H_{28}CO_2(OTMS)_2$ hydroxycarbonyl product isomers (m/z 454). Figure insets in panels (a – f) show the ion fragmentation patterns that explain the characteristic ion peaks observed in the mass spectra. The McLafferty rearrangement and H rearrangement are labeled as “ML” and “H rearrang.” respectively. Prominent fragment ion peaks that could not be identified are indicated by *. In panels (a – f), the m/z 364 fragment ion is formed from the loss of HOTMS. In panel (b), the m/z 383 fragment ion peak is formed from the loss of $C_6H_{13}O_2Si$. In panel (c), the m/z 160 fragment ion is formed from the cleavage of the C4-C5 bond in the carbon backbone. (g) The relative abundance of

$C_{17}H_{28}CO_2(OTMS)_2$ hydroxycarbonyl isomers formed during reaction at 10 % $[O_2]$ shown in GC×GC space (t_R^1 vs. t_R^2). Each circle represents a single isomer (whose mass spectrum is shown in panels a – f accordingly) and its relative abundance is represented by the size of the circle.